Available online at www.sciencedirect.com

ScienceDirect

IFAC PapersOnline CONFERENCE PAPER ARCHIVE

IFAC PapersOnLine 52-4 (2019) 222–227

Voltage Stability of Converter-Interfaced Energy Storage Systems ⋆

Álvaro Ortega * **Federico Milano** *

* *School of Electrical & Electronic Engineering University College Dublin, Ireland (e-mails: alvaro.ortegamanjavacas@ucd.ie; federico.milano@ucd.ie.)*

Abstract: This paper discusses the contribution of converter-interfaced energy storage devices to the voltage stability in transmission systems. To this aim, the paper presents static and dynamic voltage stability analyses based on a modified version of the well-known WSCC 9-bus, 3-machine test system. Results of the analyses, which have been compared with those of the more common Static Synchronous Compensator (STATCOM) devices, indicate that converter-interfaced energy storage systems will play a crucial role in the voltage stability of systems with high penetration of renewable energy sources.

Keywords: Voltage stability, converter-interfaced energy storage system (CI-ESS), static synchronous compensator (STATCOM), renewable energy source (RES), Hopf bifurcation.

1. INTRODUCTION

1.1 Motivation

An effective and widely implemented solution to overcome voltage instability is the installation of local sources of reactive power distributed over the network. The Voltage-Sourced Converter (VSC) included in Converter-Interfaced Energy Storage Systems (CI-ESSs) can contribute to the enhancement of the voltage stability margin of the system in a similar way as Flexible AC Transmission Systems (FACTS) such as STATCOMs. The paper elaborates on this statement.

1.2 Literature Review

Voltage instability is mostly a consequence of the weakness of the network and/or the shortage of reactive power sources, rather than a specific contingency. This allows using static-analysis techniques, or dynamic simulations that span several minutes and that can simulate cascading events. These studies are referred to as *long-term voltage stability* [IEEE/CIGRE Joint Task Force on Stability Terms and Definitions (2004)].

Less commonly, another type of voltage instability may also occur in the few seconds after a large disturbance such as a short circuit. Even if no voltage collapse occurs as a consequence of the disturbance, poor dynamic voltage performance can lead to voltage oscillations in the weaker areas of the system that may provoke undesired tripping of some components [Kondragunta and WSCC Reliability Subcommittee (1994)].

Studies that discuss the contribution of STATCOMs to either long-term and short-term voltage stability of power systems with high shares of RESs abound in the literature [Kolluri (2002); Kawabe and Yokoyama (2013); Cañizares et al. (1999); Arabi and Kundur (1996); Cañizares (2000)].

1.3 Contributions

To the best of the authors' knowledge, a study that gathers and discusses all relevant aspects of the corresponding contribution of CI-ESSs in a single document has not been presented yet. This paper aims to fill this gap, and provides static and dynamic analyses of the voltage stability of transmission systems with inclusion of CI-ESSs and high RES penetration.

The paper also compares the impact of CI-ESSs on the system voltage stability with that of STATCOM devices. Studies show that saturation of certain quantities of the CI-ESS can lead to some kinds of instabilities or, in some other cases, compromise the overall response of the system [Xin et al. (2016); Ortega and Milano (2015)].

1.4 Organization

The paper is organised as follows. Section 2 briefly describes the different kinds of voltage stability analysis of transmission systems proposed in [IEEE/CIGRE Joint Task Force on Stability Terms and Definitions (2004)]. Section 3 provides the models of the STATCOM and the CI-ESS, as well as their controllers, considered in this paper. A case study based on the well-known WSCC 9-bus, 3-machine benchmark system is presented in Section 4. Finally, Section 5 draws conclusions, and outlines future work directions.

⋆ This material is based upon works funded by European Union's Horizon 2020 research and innovation programme under grant agreement No. 727481. F. Milano is also funded by the Science Foundation Ireland, under grant No. SFI/15/IA/3074.
The opinions, findings, conclusions and recommendations expressed in this work are those of the authors and do not necessarily reflect the views of the European Union or Science Foundation Ireland. The European Commission and Science Foundation Ireland are not responsible for any use that may be made of the information that this work contains.

10.1016/j.ifacol.2019.08.187

2. VOLTAGE STABILITY ANALYSIS OF TRANSMISSION SYSTEMS

A common approach to study the long-term voltage stability of a system is by means of static analysis by observing the active power vs. voltage characteristics (often called *pv* curves, or informally, *nose curves* due to their characteristic shape) [Western Power Reserve Work Group (RRWG) (1998)]. *pv* curves are generated by plotting the power flow solutions of the network for different loading levels, which is used to parametrically increase all load powers with respect to the system base-case conditions.

Another long-term, small-signal voltage stability approach implies the use of dynamic models of power system devices and controllers. This method, used for example in modal analysis, implies the study of the eigenvalues of the Jacobian matrix of the system, or a reduced version of such a matrix that considers only the equations of the bus active and reactive power injections [Gao et al. (1992); Chakravorty and Patra (2016)].

The fast response of STATCOMs and CI-ESSs has been proven to greatly improve the dynamic voltage performance and, consequently, the short-term voltage stability of the grid [Kolluri (2002); Kawabe and Yokoyama (2013)]. The capability of CI-ESSs to effectively flatten voltage oscillations due to disturbances such as wind perturbations, and reduce the voltage drops due to line outages and short circuits, is studied through time domain simulations.

3. VOLTAGE CONTROL OF CONVERTER-INTERFACED REACTIVE POWER SOURCES

This section presents the scheme of the voltage control of CI-ESSs and STATCOM devices, as well as of the main device responsible of providing such a control, namely the Voltage Sourced Converter (VSC).

The general configuration in the dq-reference frame of the two converter-interfaced devices discussed in this paper is presented in Fig. 1 [Ortega and Milano (2016)]. The connection of a STATCOM device and a CI-ESS to the main grid is the same, and is based on the VSC, whose scheme coupled to the VSC inner current-control loop is shown in Fig. 2 [Yazdani and Iravani (2010); Chaudhuri et al. (2014)].

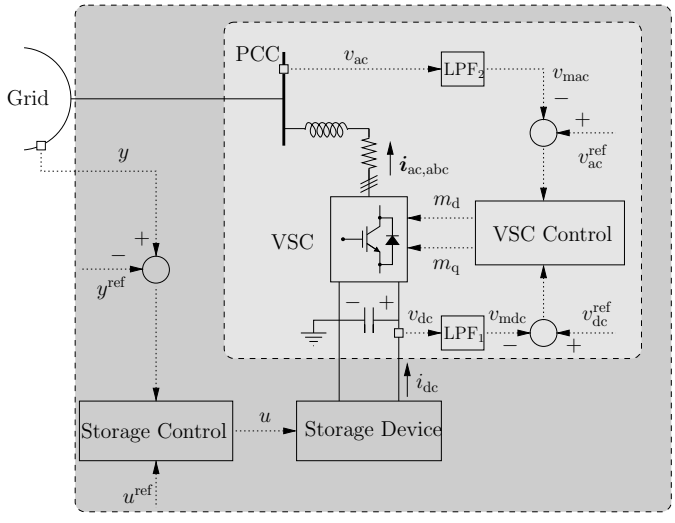

Fig. 1. Overall scheme of a converter-interfaced reactive power source connected to the AC grid. Light gray: STATCOM. Dark gray: CI-ESS.

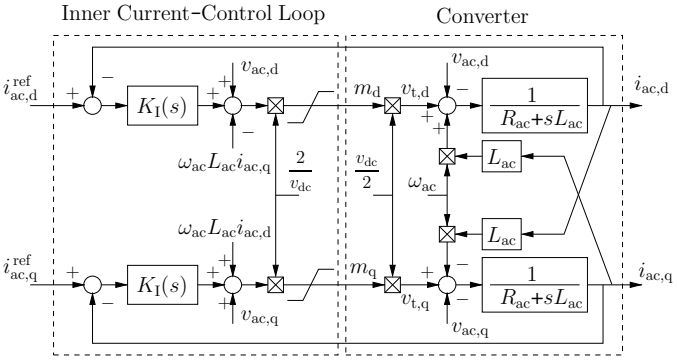

Fig. 2. Block diagram of the VSC inner current-control and converter in the dq frame.

The reference dq currents, $i_{ac,d}^{ref}$ and $i_{ac,q}^{ref}$, are imposed by the decoupled outer voltage-control loop depicted in Fig. 3.

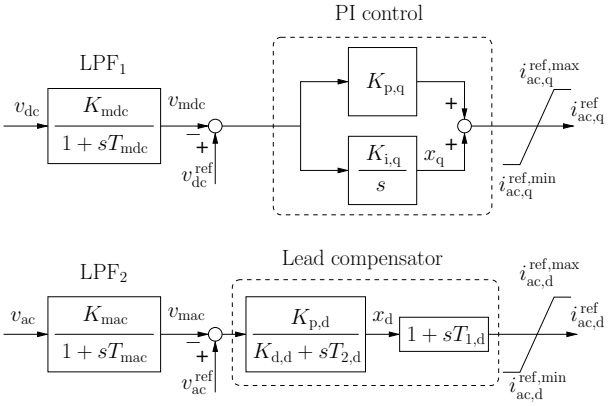

Fig. 3. Outer DC- and AC-voltage controllers of the VSC.

4. CASE STUDY

Figure 4 shows a modified version of the well-known WSCC 9-bus, 3-machine test system originally presented in [Sauer and Pai (1998)].

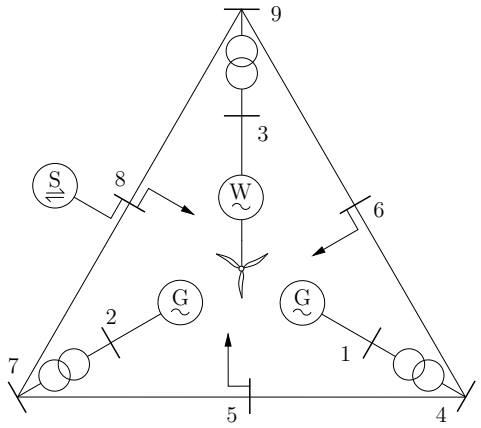

Fig. 4. Modified WSCC 9-bus, 3-machine system.

The WSCC 9-bus system is often utilized for transient and frequency stability analysis. While focusing on voltage stability, this network is considered in this case study, as the main transient effect of the BES is its ability to exchange active power with the grid. As any other network, however, the WSCC 9-bus system shows a maximum loading condition and, consequently, can face voltage collapse. This network is thus as good as any other system to carry out voltage stability analysis.

Since the original WSCC system is fairly symmetrical, some modifications to the base-case data are introduced with the aim of creating a weak area, i.e., the bus where the wind turbine is installed and neighbouring buses. The modifications are as follows.

- The power base of the system has been reduced by 3 times, i.e., $s_n = 33.3$ MVA.
- The voltage of all transmission lines has been reduced by $\sqrt{3}$ times.
- The synchronous machine at bus 3 has been replaced by a wind power plant of the same capacity. The wind power plant is modelled as an aggregation of 18 fifth-order doubly-fed induction generators with optimal cubic MPPT approximation, first-order primary voltage regulation and static turbine governor.
- In time domain simulations, the wind follows a stochastic, exponentially autocorrelated Weibull-distributed process modelled as a set of stochastic differential equations [Zárate Miñano and Milano (2016)].
- Consistently with time scales and conventional assumptions, loads are modelled as constant PQ for the continuation power flow analysis and as constant impedances for time domain simulations.
- The voltage at the synchronous machine buses is reduced by 2% with respect to the base case.
- The system includes a secondary frequency controller (AGC) with gain $K_o = 2$.
- When considered, the CI-ESS and the STATCOM device are connected to bus 8 through a 133/21 kV transformer.
- The CI-ESS is a Battery Energy Storage (BES) modelled using the well-known Sheperd's model [Shepherd (1965); Ortega and Milano (2016)].
- The active power rating of the BES is 3.2 MW.
- The CI-ESS active power control is designed to regulate the frequency at the point of common coupling (PCC) with the grid, i.e., the frequency at bus 8. The frequency is estimated by means of a phase-locked loop (PLL) device [Cole (2010)].

Two main scenarios are considered. First, Subsection 4.1 discusses the long-term voltage stability of the WSCC system using both static and dynamic models of the power system devices and controllers. Then, the short-term voltage stability of the dynamic model of the WSCC system is studied through time domain simulations in Subsection 4.2.

All simulations included in the paper are obtained using the Python-based software tool Dome [Milano (2013)]. The Dome version utilised is based on Ubuntu Linux 18.04, Python 3.6.7, CVXOPT 1.2.2, KLU 1.3.8, and MAGMA 2.2.0.

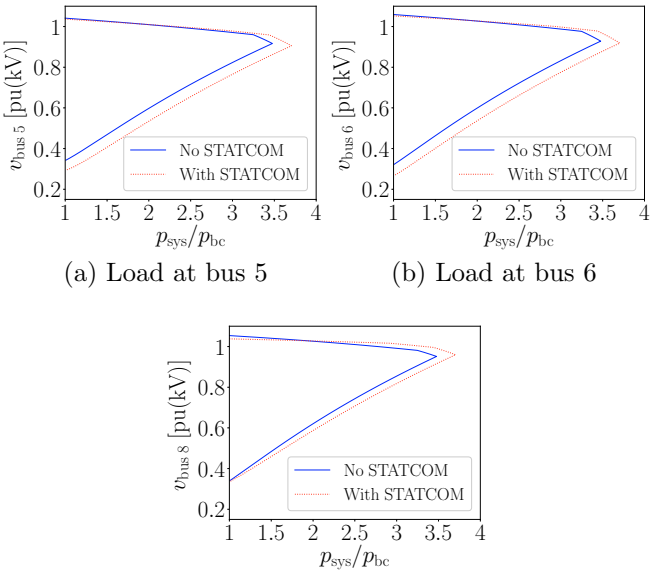

(a) Load at bus 5 (b) Load at bus 6

(c) Load at bus 8

Fig. 5. *pv* curves at the load buses of the modified WSCC 9-bus system with and without a STATCOM. The x-axis represents the ratio between the loading level of the system, p_{sys}, and the base-case condition, p_{bc}.

4.1 Long-Term Voltage Stability

The *pv* curves of the three loads of the modified WSCC system of Fig. 4 with and without a 20 MVAr STATCOM at bus 8 are shown in Fig. 5. Reactive power limits of the generators are of ±42 and ±55 MVAr for the synchronous machines at buses 1 and 2, respectively, and of ±10 MVAr for the wind power plant at bus 3.

In steady state, the active power output of a CI-ESS is null, as generation and demand are balanced. Therefore, the static models of a STATCOM device and a CI-ESS coincide. In particular, the STATCOM is modelled as a constant active power, with $p_{\text{ac}} = 0$, and constant voltage if the reactive power is within the limits, and as a constant active and reactive power with $p_{\text{ac}} = 0$ and $q_{\text{ac}} = \pm 20$ MVAr, otherwise.

Figure 5 shows that the STATCOM allows increasing the loading level of the system up to 3.7 times the base-case conditions, as opposed to maximum ratio of 3.47 of the case without STATCOM, i.e., a 6.56% relative increase. The STATCOM also maintains the voltage of the load at the PCC (i.e., bus 8) almost at a constant value up to near the point of collapse.

The impact of the STATCOM on the voltage stability is more relevant in the event of the outage of one of the transmission lines, as represented in Fig. 6, where the *pv* curves are computed considering that the line connecting buses 4 and 5 has been disconnected. After the line outage, the maximum ratio $p_{\text{sys}}/p_{\text{bc}}$ decreases to 2.64 and 2.86 without and with the STATCOM, respectively, i.e., a 8.24% relative increase. The outage of the line implies approximately a 24% reduction with respect to the fully connected system. Similar conclusions can be drawn considering voltage-dependent load models.

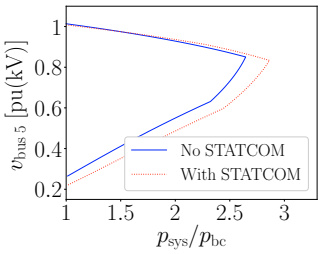

(a) Load at bus 5

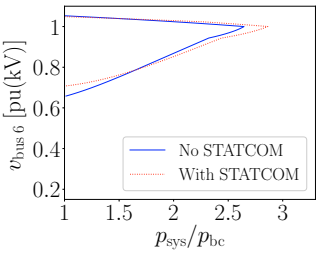

(b) Load at bus 6

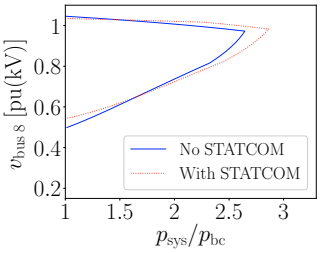

(c) Load at bus 8

Fig. 6. *pv* curves at the three load buses of the modified WSCC system with and without a STATCOM. The line between buses 4 and 5 is disconnected.

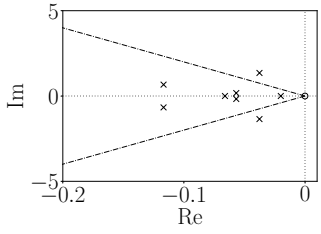

(a) WSCC system without BES. $p_{\text{sys}}/p_{\text{bc}} = 1.0$

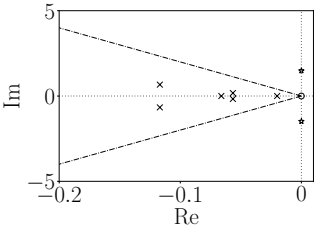

(b) WSCC system without BES. $p_{\text{sys}}/p_{\text{bc}} = 1.673$

Fig. 7. Eigenvalue loci of the rightmost eigenvalues of the WSCC system. Dash-dot lines indicate 5% damping.

A second long-term, small-signal voltage stability analysis is presented below which considers dynamic models of the power system devices and controllers of the WSCC system. For this study, the increasing loading level of the system is compensated by the two synchronous machines of the system, as it is assumed that no more active and reactive power can be extracted from the wind power plant.

Figure 7 shows the rightmost eigenvalues of the WSCC system for two loading levels: (i) the base-case condition, and (ii) 1.673 times p_{bc}. It can be seen that, for $p_{\text{sys}}/p_{\text{bc}} \geq 1.673$, a complex pair of eigenvalues, which is related to the states $e'_{r,\text{q}}$ and v_e of the synchronous machine at bus 1, crosses the imaginary axis, thus becoming unstable modes. The Hopf bifurcation Seydel (2010) occurring when $p_{\text{sys}}/p_{\text{bc}} = 1.673$ prevents the operation of the system at higher loading levels which, from the static analysis above, could be up to 3.47.

The installation of additional sources of reactive power such as STATCOM and BES devices allows increasing the loading level of the system beyond the critical value of 1.673 times the base-case condition, as these devices shift to the left the pair of eigenvalues that cause the Hopf bifurcation. This is shown in Fig. 8 for the scenarios where

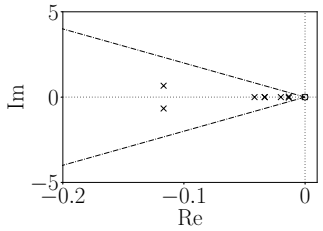

(a) WSCC system with BES. $p_{\text{sys}}/p_{\text{bc}} = 1.673$

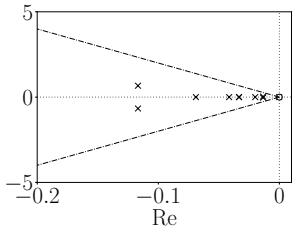

(b) WSCC system with BES. $p_{\text{sys}}/p_{\text{bc}} = 2.5$

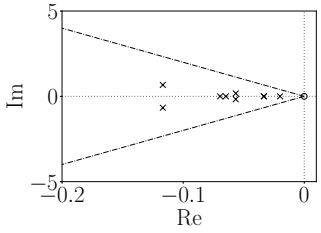

(c) WSCC system with STATCOM. $p_{\text{sys}}/p_{\text{bc}} = 2.5$

Fig. 8. Eigenvalue loci of the rightmost eigenvalues of the WSCC system with a BES and a STATCOM. Dash-dot lines indicate 5% damping.

a BES or a STATCOM device is connected to bus 8. In this case, the reactive power rate of both devices is set to 20 MVAr.

In Fig. 8(a), the inclusion of a BES system shifts the eigenvalues that caused the Hopf bifurcation in the system to a value of $-0.396 \pm j0.924$. The 6 rightmost eigenvalues are in this case within the 5% damping thresholds, being the eigenvalue #7, which is related to the rotor speeds of the two synchronous machines, the first one that shows poorly damped behaviour ($-0.288 \pm j10.59$). This result holds even for larger loading levels, as shown in Fig. 8(b) for $p_{\text{sys}}/p_{\text{bc}} = 2.5$. In this case, the aforementioned poorly damped eigenvalues are $-0.249 \pm j10.76$. The real part of such eigenvalues is still about an order of magnitude larger than the dominant modes of the system.

Finally, from the voltage stability point of view, no relevant differences can be observed between installing a BES or a STATCOM device, as observed from comparing Figs. 8(b) and 8(c). This is an expected result due to the similar configuration of the reactive power support of both devices. This result also indicates that the active power support of the BES does not compromise the voltage stability of the overall system for relatively large loading levels.

4.2 Short-Term Voltage Stability

This section studies, through time domain simulations, the short-term dynamic response of the modified WSCC system with inclusion of CI-ESSs. Two scenarios are presented to analyse both small- and large-disturbance voltage stabilities. The reactive power rate of the CI-ESS and the STATCOM device used in the comparison is 3.2 MVAr. This value is chosen with the aim of analysing the impact

of hitting the current limits included in the schemes shown in Fig. 3.

Small disturbances are modelled as stochastic wind perturbations that follow a Weibull distribution with exponential autocorrelation. The response of the WSCC system following such perturbations is shown in Fig. 9. Figure 9(a) depicts the voltage at bus 8, i.e., the PCC with the CI-ESS or the STATCOM device. Wind perturbations create sustained voltage oscillations which, despite having relatively small magnitude, can deteriorate certain components of the load connected at the bus, and/or compromise their operation.

The average value of the voltage varies substantially with respect to the operating condition during the simulation. The inclusion of a CI-ESS or a STATCOM in the system allows reducing to a great extent the voltage oscillations, and keeps the average voltage close to its reference value. While both the CI-ESS and the STATCOM device show similar performance, the ability of the CI-ESS to also provide active power control leads to a more efficient voltage regulation with respect to the STATCOM, as it requires less reactive power support and proved better voltage response (see Fig. 9(c)).

Finally, despite the local nature of the voltage control from both devices, their effect can be observed also at the system level, as shown in Fig. 9(b), which includes the trajectories of the voltage at the load bus 6. Such a voltage shows a better profile when a CI-ESS or a STATCOM is included in bus 8.

The last scenario presented in this paper studies large-disturbance voltage stability. With this aim, the outage of the line connecting buses 4 and 5 is simulated at $t = 1$ s, and simulation results are shown in Fig. 10. The wind turbine is assumed to include a low-voltage ride-through protection that prevents its disconnections after the disturbance. Installing a BES allows reducing the voltage sag by about 30%. Moreover, after the voltage sag, large-amplitude voltage oscillations lasting about 10 s can be observed in the case without additional reactive power support. Such oscillations are remarkably flattened with both the BES and the STATCOM devices.

The steady-state value of the voltage at the PCC is also kept at its reference value, as opposed to the base case which shows a slightly lower value in steady state. Similarly to the small-disturbance scenario, the effect of installing a local reactive power source are observed in the overall system, as shown in Fig. 10(b). Finally, Fig. 10(c) shows that the saturation of the current of the outer-voltage control of the VSC, while limiting its regulation capability, does not deteriorate the voltage response of the overall system.

5. CONCLUSIONS

This paper presents a detailed analysis of the impact of CI-ESSs on the voltage stability of transmission systems with large penetration of RESs. The performance of CI-ESSs is duly compared with that of more conventional STATCOM devices. Several relevant aspects of voltage stability analysis are studied and discussed, including long-term, steady-state analysis, as well as short-term dynamic

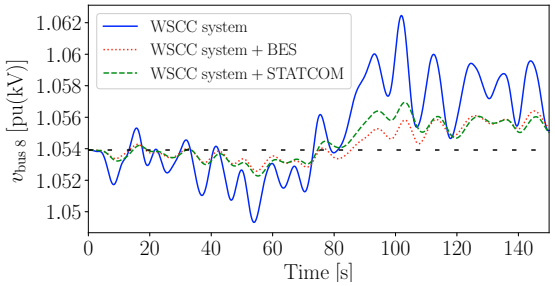

(a) Voltage at the PCC

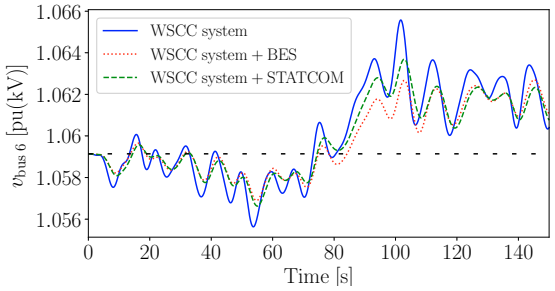

(b) Voltage at the load bus 6

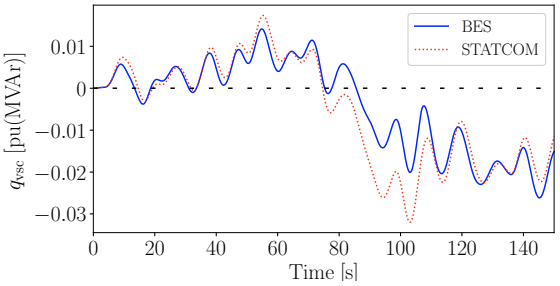

(c) Reactive power output of the VSC

Fig. 9. Response of the WSCC system following stochastic wind variations.

simulations, based on a modified model of the well-known WSCC 9-bus system.

Simulation results indicate that the inclusion of fast-responding reactive power support improve every aspect of the voltage stability studied as it: (i) increases the maximum loading level of the system; (ii) improves the small-signal stability for large loading conditions; (iii) reduces voltage oscillations due to perturbations such as those caused by the wind; (iv) maintains the voltage at the bus of connection at its reference value for a variety of disturbances, and (v) reduces the voltage sag resulting from large disturbances such as line outages and faults.

Other less intuitive results have also been observed in this paper: (i) CI-ESSs provide more efficient voltage regulation than STATCOM devices thanks to their capability to provide simultaneously active and reactive power support; (ii) the dynamics of the energy storage device and its active power control do not deteriorate the small-signal voltage stability of the system even for large loading levels; (iii) current saturations of the power converter do not appear to compromise the short-term voltage stability of the overall system, at least in the considered scenarios; (iv) the impact of the local voltage support provided by CI-ESSs can be observed at a system level.

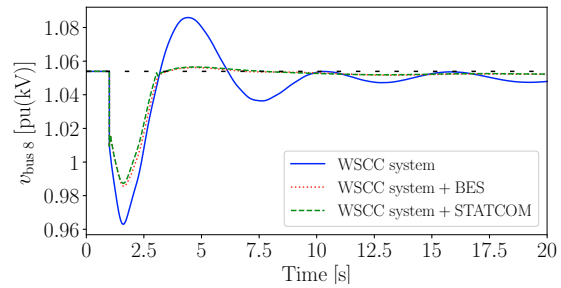

(a) Voltage at the PCC

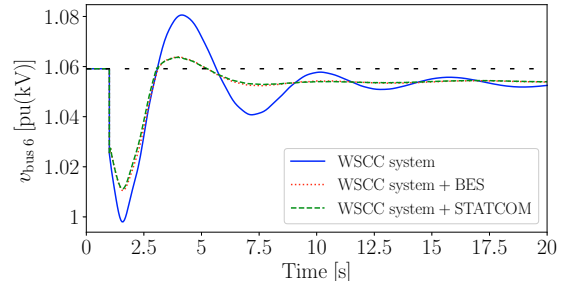

(b) Voltage at the load bus 6

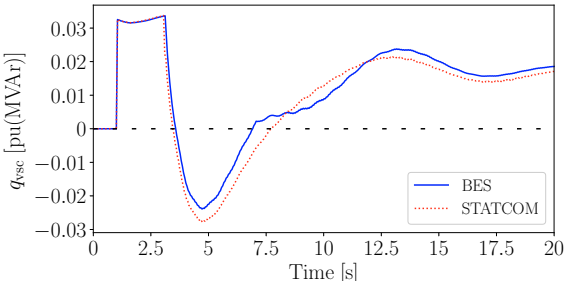

(c) Reactive power output of the VSC

Fig. 10. Response of the WSCC system following a line outage.

Future work will focus on the study of the stability of CI-ESSs included in microgrids. Low X/R ratios of microgrids feeder lines imply strong couplings between voltage and frequency. The capability of CI-ESSs to simultaneously regulate the frequency and voltage at the PCC in a very short time frame makes these devices excellent candidates to cope with such couplings.

REFERENCES

Arabi, S. and Kundur, P. (1996). A versatile FACTS device model for powerflow and stability simulations. *IEEE Transactions on Power Systems*, 11(4), 1944–1950.

Cañizares, C., Corsi, S., and Pozzi, M. (1999). Modeling and implementation of TCR and VSI based FACTS controllers. Internal report, ENEL and Politecnico di Milano.

Cañizares, C.A. (2000). Power flow and transient stability models of FACTS controllers for voltage and angle stability studies. In *2000 IEEE Power Engineering Society Winter Meeting. Conference Proceedings*, volume 2, 1447–1454 vol.2.

Chakravorty, M. and Patra, S. (2016). Voltage stability analysis using conventional methods. In *2016 International Conference on Signal Processing, Communication, Power and Embedded System (SCOPES)*, 496–501.

Chaudhuri, N.R., Chaudhuri, B., Majumder, R., and Yazdani, A. (2014). *Multi-terminal Direct-current Grids: Modeling, Analysis, and Control*. John Wiley & Sons.

Cole, S. (2010). *Steady-State and Dynamic Modelling of VSC HVDC Systems for Power System Simulation*. Ph.D. thesis, Katholieke Universiteit Leuven.

Gao, B., Morison, G.K., and Kundur, P. (1992). Voltage stability evaluation using modal analysis. *IEEE Transactions on Power Systems*, 7(4), 1529–1542.

IEEE/CIGRE Joint Task Force on Stability Terms and Definitions (2004). Definition and classification of power system stability. *IEEE Trans. on Power Systems*, 19(2), 1387–1401.

Kawabe, K. and Yokoyama, A. (2013). Study on short-term voltage stability improvement using batteries on extra-high voltage network. In *Proceedings of the IEEE Grenoble Conference*, 1–3.

Kolluri, S. (2002). Application of distributed superconducting magnetic energy storage system (D-SMES) in the entergy system to improve voltage stability. In *Proceedings of the IEEE PES Winter Meeting*, volume 2, 838–841.

Kondragunta, J. and WSCC Reliability Subcommittee (1994). Supporting document for reliability criteria for transmission system planning. Technical report, Western Systems Coordinating Council (WSCC).

Milano, F. (2013). A Python-based software tool for power system analysis. In *Proceedings of the IEEE PES General Meeting*.

Ortega, Á. and Milano, F. (2015). Design of a control limiter to improve the dynamic response of energy storage systems. In *Proceedings of the IEEE PES General Meeting*.

Ortega, Á. and Milano, F. (2016). Generalized model of VSC-based energy storage systems for transient stability analysis. *IEEE Trans. on Power Systems*, 31(5), 3369–3380.

Sauer, P.W. and Pai, M.A. (1998). *Power System Dynamics and Stability*. Prentice Hall, Upper Saddle River, NJ.

Seydel, R. (2010). *Practical Bifurcation and Stability Analysis*. Springer Science & Business Media, New York, US, third edition.

Shepherd, C.M. (1965). Design of primary and secondary cells II. An equation describing battery discharge. *Journal of the Electrochemical Society*, 112(7), 657–664.

Western Power Reserve Work Group (RRWG) (1998). Voltage stability criteria, undervoltage load shedding strategy and reactive power reserve monitoring methodology. Technical report, Western Electricity Coordinating Council (WECC).

Xin, H., Huang, L., Zhang, L., Wang, Z., and Hu, J. (2016). Synchronous instability mechanism of P-f droop-controlled voltage source converter caused by current saturation. *IEEE Transactions on Power Systems*, 31(6), 5206–5207.

Yazdani, A. and Iravani, R. (2010). *Voltage-Sourced Converters in Power Systems – Modeling, Control and Applications*. Wiley-IEEE Press.

Zárate Miñano, R. and Milano, F. (2016). Construction of SDE-based wind speed models with exponentially decaying autocorrelation. *Renewable Energy*, 94, 186 – 196.